HHS Public Access

Author manuscript

Magn Reson Med. Author manuscript; available in PMC 2021 March 01.

Published in final edited form as:

Magn Reson Med. 2020 March ; 83(3): 1066–1080. doi:10.1002/mrm.27972.

Quantification of Whole-Brain Oxygenation Extraction Fraction and Cerebral Metabolic Rate of Oxygen Consumption in Adults with Sickle Cell Anemia using Individual T_2-based Oxygenation Calibrations

Wenbo Li[1,2], **Xiang Xu**[1,2], **Peiying Liu**[1], **John J. Strouse**[3,4], **James F. Casella**[3], **Hanzhang Lu**[1], **Peter C.M. van Zijl**[1,2], **Qin Qin**[1,2]

[1]The Russell H. Morgan Department of Radiology and Radiological Science, Division of MR Research, Johns Hopkins University School of Medicine, Baltimore, MD, USA

[2]F.M. Kirby Research Center for Functional Brain Imaging, Kennedy Krieger Institute, Baltimore, MD, USA

[3]Department of Pediatrics, Division of Pediatric Hematology, Johns Hopkins University School of Medicine, Baltimore, MD, USA.

[4]Division of Hematology, Duke University, Durham, NC, USA

Abstract

Purpose: To evaluate different T_2-oxygenation calibrations for estimating venous oxygenation in people with sickle cell anemia (SCA).

Methods: Blood T_2 values were measured at 3T in the internal jugular veins of 12 healthy volunteers and 11 SCA participants with no history of stroke, recent transfusion, or renal impairment. T_2-oxygenation relationships of both sickled and normal blood samples were calibrated individually and compared with values generated from published models. After converting venous T_2 values to venous oxygenation, whole-brain oxygen extraction fraction (OEF) and cerebral metabolic rate of oxygen ($CMRO_2$) were calculated.

Results: Sickle blood samples' oxygenation values (Y) calculated from our individual calibrations agreed well with measurements using a blood analyzer, while previous T_2 calibrations based on normal blood samples showed 13–19% underestimation. Meanwhile, Y values calculated from previous grouped T_2 calibration for sickle blood agreed well with experimental measurement on averaged values, but showed up to 20% variation for several individual samples. Using individual T_2 calibrations, the whole-brain OEF and $CMRO_2$ of SCA participants were 0.38+/−0.08 and 172+/−42μmol/min/100g, respectively, which were comparable to those values measured on normal volunteers.

Conclusion: Our results confirm that sickle blood T_2 values not only depend on Hct and Y, but also on other hematological factors. The individual T_2 calibrations minimized the effect of

Corresponding author: Wenbo Li, PhD, Department of Radiology, Johns Hopkins University School of Medicine, F.M. Kirby Research Center for Functional Brain Imaging, Kennedy Krieger Institute, 707 N. Broadway, Baltimore, MD, 21205, wli47@jhmi.edu.

heterogeneity of sickle blood between different SCA populations and improved the accuracy of T_2-based oximetry. The measured OEF and $CMRO_2$ of this group of SCA participants were found to not differ significantly from those of healthy people.

Keywords

Blood T_2; OEF; $CMRO_2$; Sickle cell disease; HbS; T_2 oximetry

INTRODUCTION

Sickle cell anemia (SCA) is an inherited blood disorder that is characterized by the presence of two genes for hemoglobin S (HbS). It not only causes the abnormal shape (sickled) of erythrocytes, but also significant hemolysis. This decreases the hematocrit (Hct, the volume fraction of erythrocytes in blood), and thus the arterial oxygen content. In response to this low arterial oxygen content, autoregulation causes elevated cerebral blood flow (CBF) to normalize oxygen delivery in SCA[1–9]. When oxygen delivery can no longer be maintained, the oxygen extraction fraction (OEF) increases to preserve oxygen delivery, very similar to acute ischemia in non-SCA populations[10–15]. As such, OEF may be a marker of inadequate cerebrovascular reserve in SCA and an indicator of increased risk of cerebral dysfunction and ischemia induced due to the lack of tissue oxygen[8,16]. Positron emission tomography (PET) is able to measure CBF, oxygen extraction fraction (OEF) and cerebral oxygen metabolic rate ($CMRO_2$)[17], but is invasive, expensive and not widely available. Oxygen-15 PET has been applied to study the cerebral oxygen utilization of SCA patients and no significant differences of OEF and $CMRO_2$ were found when comparing a small group of patients with SCA and normal adults[2].

MRI oximetry using either T_2*[18–23] or T_2[24–33] provides an alternative to measure OEF non-invasively. This approach is based on the principle that hemoglobin changes its magnetic property from paramagnetic to diamagnetic when binding oxygen, thereby altering water T_2 and T_2*. A T_2* oximetry method based on asymmetric spin echo (ASE) acquisition[34] has been used to measure the OEF in children with SCA[7,35,36], however, increased iron deposition in tissue of SCA patients would reduce tissue T_2*[37] and this could lead to bias and limit its application in SCA.

The T_2 oximetry method could alleviate this problem, as it is independent of the tissue environment. The blood T_2 value measured from a large vein can be converted to oxygenation (Y) through a predefined calibration based on the dependence of T_2 on both Y and Hct[24–32]. Therefore, a proper calibration is crucial to obtain a reliable oxygenation measurement. Previously, sickle blood was assumed to have blood T_2 calibration similar to normal blood[38]. Using an existing T_2 calibration developed from normal blood[39], elevated OEF values were reported for the SCA volunteers, both with blood transfusion and without blood transfusion[38,40,41], however, another study[42] measured T_2 values of sickle blood samples, showing a ~20% shorter T_2 value of sickle blood than T_2 value of normal blood at the same Hct and Y. Based on these in vitro data, they developed a group-based T_2 calibration specific for sickle blood and observed reduced OEF and $CMRO_2$ of SCA patients[42].

The discordant findings of OEF among SCA patients from the few MRI studies[38,40–42] is perplexing. One possibility explaining the discrepancy could be the heterogeneity of sickled blood composition between different SCA participants. Sickled blood contains erythrocytes with normal shape (biconcave disk) in addition to those reversibly and irreversibly sickled. The percentage of these sickled erythrocytes highly varies depending on multiple factors, such as the concentration of HbS and fetal hemoglobin (HbF) in erythrocytes, which differs among individual erythrocytes in the same SCA patient[43,44]. It has been shown that blood T_2 values also depend on the shape of erythrocyte[45]. Meanwhile, aggregation of HbS under deoxygenated conditions also shortens blood T_2 values[46]. This dependence of T_2 values of blood on factors other than Y and Hct should be taken into account when studying sickled blood and indicate that calibrations from normal blood may not be correct.

To take into account the heterogeneity of sickle blood T_2-Y relationships between different SCA participants, we measured the Y dependence of sickle blood T_2 for each subject and used the individual T_2-Y calibration to convert the venous T_2 value to Y_v for each SCA participant. Using this method, we determined whole-brain OEF and $CMRO_2$ for 11 SCA participants and compared the results with those obtained from 12 healthy participants.

Methods

In Vivo Experiments

Experiments were performed on a 3T Philips Achieva scanner (Philips Medical Systems, Best, Netherlands) using a 32-channel head coil for signal reception and the body coil for radiofrequency transmission. Twelve healthy volunteers (35 ± 7 yrs; 6M / 6F; Hct: 0.42 ± 0.04) and eleven subjects with SCA with no history of stroke, recent transfusion, or renal impairment (25 ± 7 yrs; 4M / 7F; Hct: 0.27 ± 0.04; sickle hemoglobin (HbS): 82.7% ± 6.4%; fetal hemoglobin (HbF): 8.7% ± 4.3%) participated in this study after providing informed written consent in accordance with local Institutional Review Board guidelines.

For the scan planning, phase-contrast magnetic resonance angiogram (PC-MRA) survey images were acquired in both sagittal and coronal planes to visualize the location and orientation of internal jugular veins (IJVs), using the acquisition parameters: slab thickness = 50 mm, TR/TE = 20/6.3 ms, FOV = 250 × 250 mm^2, and scan matrix of 256 × 128 (acquisition time: 20 s × 2).

Venous blood T_2 was measured in the right IJV using a 5 mm axial slice perpendicular to it for localization, using an MRI protocol with a T2prep module that played out with five different echo times (TEprep = [20, 40, 80, 120, 160] ms) and a constant inter-echo spacing of 10 ms as described previously[26]. Composite refocusing pulses, $90°_x180°_y90°_x$, and MLEV-16 phase cycling were used in the T2prep module for reliable refocusing *in vivo* and the corrected echo times (TE_{corr} = [18.3, 36.5, 73.0, 109.6, 146.1] ms) were used to take into account of the pulse length of the refocusing composite pulse[26,47]. Following the acquisition, a tailored hard-pulse train[48] for global saturation (65°, 83°, 143°, 162°) resets the remaining magnetization to zero, with a fixed delay of 2 sec to ensure a constant initial longitudinal magnetization before T2prep module. The acquisition parameters were: FOV = 169 ×169 mm^2, in-plane resolution = 0.8 × 0.8 mm^2, TR/TE/FA = 13 ms/ 7.6 ms/ 50°,

sensitivity encoding (SENSE) factor = 2, multi-shot turbo field echo (TFE) acquisition with 7 shots and TFE factor = 15, the acquisition window for each shot was about 195 ms. The total acquisition time was 1 min.

Although the SCA participants have faster flow than normal participants we studied previously[26], the T_2 preparation (CPMG) module in this protocol used global refocusing pulses, which means all venous blood in the brain experienced the same T_2 decay during the T_2 preparation module. This T_2 preparation module was short, varying from 20ms to 160ms. During this short time, all the blood in the imaging plane experienced the same T_2 preparation; therefore, there should be not significant flow effect on our T_2 measurement.

To evaluate the reliability of this T_2 protocol [26] on SCA participants, we recruited three SCA participants, and repeatedly measured T_2 values at IJV three times consecutively during the same session.

In order to obtain the baseline whole-brain CBF, phase-contrast MRI (PC-MRI) was used to measure the blood flow rates at the bilateral internal carotid arteries (ICA) and vertebral arteries (VA). Four runs of 2D PC MRI were planned perpendicular to the corresponding arteries as described previously [49] with the acquisition parameters: slice thickness = 5 mm, FOV = 200 × 200 mm^2, in-plane resolution = 0.5 × 0.5 mm^2, TR/TE/FA = 19 ms / 9 ms / 15°. The encoding velocities were 60 cm/s (ICA) and 40 cm/s (VA) for healthy volunteers and 100 cm/s (ICA) and 60 cm/s (VA) for SCA participants, respectively. In addition, a T_1-weighted magnetization prepared rapid gradient-echo (MPRAGE) scan was added for brain gray matter volume estimation to obtain a unit volume CBF value, using the acquisition parameters: TR/TE/FA = 12 ms / 3.2 ms / 9°, shot interval = 1720ms, inversion time (TI) = 1100 ms, FOV = 220 × 220 × 180 mm^3, nominal voxel size of 1.1 mm isotropic, SENSE factor = 2 × 2, duration of 5 min.

In Vitro Experiments

Four 4 mL-tubes of blood were collected from the antecubital vein of all participants right before their MRI scans. Two tubes of blood anticoagulated using EDTA were sent to the hospital's pathology laboratory to have a complete blood count (CBC) for all subjects and a hemoglobin variant quantification for SCA subjects only. The other tubes of blood were anticoagulated with lithium heparin and stored at room temperature. They were used for in vitro experiments on the same day as the in vivo measurements. Following a previous protocol[50], the oxygenation of the blood samples was first adjusted using air or N_2 gas moisturized by PBS buffer. Then the blood samples (2~3mL) were sealed in a tube with a diameter of 1 cm and equilibrated at 37.8 °C water bath for 5 min before the MRI measurement. During the MRI experiment, the blood tube was placed in a 1L water bath (37.8 °C) to maintain the temperature. After MRI experiments, the oxygenations of blood samples were immediately measured using a blood analyzer equipped with co-oximetry (ABL800, Radiometer). For each sickle blood sample, 5–7 oxygenations were prepared to cover the oxygenation range from ~50% to ~100%.

It is worthy to note that because the erythrocytes' volume changes at different oxygenations, the Hct definition used in the blood analyzer (i.e. Hct is equal to the total hemoglobin concentration divided by 33.2g/dL), was used in this study.

A two-channel shoulder coil was used for signal reception in the in vitro experiments. The T_2 of blood samples were measured using a pulse sequence with a T2prep module similar to the in vivo experiments. Two-shot TFE (TR/TE/FA = 15 ms/2.5 ms/8°, TFE factor = 20) was used to acquire a 2D image of 3 mm thick with FOV of 64 × 120 mm^2 and a resolution of 1 × 2 mm^2. A sagittal slice was acquired, which was used to check whether there was erythrocyte settlement by evaluating the blood T_2 values vertically (Supporting Information Fig. S1)[50]. The scan time was 27 s for each oxygenation level. The complete MRI measurement, including placing the sample into MRI scanner, survey scan and T_2 scan, was controlled to be under 2 min to prevent the settling of erythrocytes.

Data Analysis

Matlab (MathWorks, Natick, Massachusetts, USA) was used for data processing. T_2 values were obtained from mono-exponential fitting of the MRI signal as a function of effective TE at both in vivo and in vitro experiments.

To establish an analytical relationship between Y and T_2 for each individual, the in vitro T_2 data for the blood samples from the same volunteer with different oxygenation levels were fitted to an empirical model[28]:

$$R_2 = 1/T_2 = A_1 \times (1 - Y)^2 + A_2 \quad \text{Eq. 1}$$

where R_2 was the measured T_2 relaxation rate ($1/T_2$) and A_1 and A_2 were the fitting parameters which are characteristic for each volunteer.

In addition to the individual T_2 calibration, previously reported T_2 calibrations for normal blood [39,51] and sickle blood[42] were used to calculate Y, and the values (Y_{Cal}) from different calibration approaches were compared with the observed Y ($Y_{Observe}$) obtained from the blood analyzer.

Note that the previous T_2 calibrations[39,42,51] were built from apparent T_2 ($T_{2,app}$) without correcting the pulse width (pw) of refocusing pulses in a CPMG sequence[47]. To compare different T_2 calibrations, our measured corrected T_2 ($T_{2,corr}$) values that take into account the refocusing pulse lengths should be converted to the $T_{2,app}$ values that were used in the previous T_2 calibrations. Since the inter-echo spacing between refocusing pulses (τ_{cp}) and pw of refocusing pulses used in the previous experiments[39,50,51] were the same (τ_{cp}: 10 ms; pw: ~1.74 ms), the relationship between $T_{2,app}$ and $T_{2,corr}$ can be calculated as

$$T_{2,app} = T_{2,corr}/k \quad \text{Eq. 2}$$

where $k = 1 - pw/(2\times\tau_{cp}) = 1 - 1.74/(2\times10) = 0.913$ [26,47]. Using Eq.2, the $T_{2,corr}$ can be simply scaled to $T_{2,app}$ that is suitable to calculate Y using the previous T_2 calibrations[39,42,51].

The venous oxygenation (Y_v) of SCA participants was calculated by substituting the in vivo measured T_2 value in the IJV into their own T_2–Y calibration. OEF was calculated using

$$OEF = (Y_a - Y_v)/Y_a \quad \text{Eq. 3}$$

assuming an arterial blood oxygenation Y_a of 0.98.

In order to obtain baseline whole-brain CBF, the fluxes of ICAs and VAs were extracted from PC-MRI data following the method used in a previous study [49]. An ROI was drawn on each of these four main feeding arteries based on magnitude image and used to create an ROI mask. The velocity values within this ROI mask were integrated to yield the flux (mL/min) for each artery. To calculate CBF value, the image from the MPRAGE experiment was segmented using the software FSL (FMRIB software Library, Oxford University) and the brain's total parenchymal volume was estimated by the sum of gray and white matter volumes and converted to the weight of the brain using a parenchymal density of 1.06g/mL[52]. The CBF (mL/min/100g) was then calculated by normalizing the main arterial blood flux to the brain parenchymal mass.

$CMRO_2$ (μmol/min/100g) was then calculated using the equation introduced by Kety and Schmidt [53] based on the Fick principle of arteriovenous oxygen difference:

$$CMRO_2 = CaO_2 \times CBF \times OEF \quad \text{Eq. 4}$$

where CaO_2 (μmol/mL) is the arterial oxygen content which represents the amount of oxygen that a unit volume of arterial blood can carry. Considering one tetramer of hemoglobin can carry four oxygen molecules, CaO_2 is calculated based on the hemoglobin concentration in the blood (ctHb, g/L) as

$$CaO_2(\mu\text{mol/mL}) = 4 \times \frac{ctHb(g/L) \times 10^{-3} L/mL}{64.5 \times 10^3 g/mol \times 10^{-6} mol/\mu\text{mol}} \times Y_a \quad \text{Eq. 5}$$

where 64.5×10^3g/mol is the molecular weight of hemoglobin tetramer, which is the same for normal and sickle hemoglobin.

The oxygen delivering rate DO_2 (μmol/min/100g) can be calculated as

$$DO_2 = CBF \times CaO_2 \quad \text{Eq. 6}$$

An F-test was used to test the homogeneity of group variance for differences between *in vitro* measured Y and calculated Y based on different T_2 calibrations. The intraclass correlation coefficient (ICC) was calculated for three repeated T_2 measurements on each SCA participants to evaluate the reliability. The Wilcoxon rank-sum test was used to evaluate the group difference on OEF, CBF and $CMRO_2$ between healthy volunteers and SCA participants.

Results

Figs. 1a and b show representative images acquired at the shortest TE_{corr} for the in vivo and in vitro experiments from one SCA participant, respectively. The T_2 values were obtained from fitting the signal intensities in the IJV (Fig. 1c) or the blood tube (Fig. 1d) as a function of corrected TE. For *in vitro* scan of Fig. 1b, three smaller ROIs were chosen from the top to the bottom of the tube, and their T_2 values were fitted separately (Supporting Information Fig. S1) and found to be similar, from which we concluded that there was minimal erythrocyte settlement during our measurements.

The fittings (black lines) of R_2 of blood samples (black dots) from each individual SCA participant are displayed in Fig. 2 and show a quadratic dependence on the deoxygenation fraction (1-Y) (Eq. 1), similar to plots for normal blood (Supporting Information Fig. S2). When comparing these curves with previous generalized calibrations (Fig. 2), the individually measured R_2 values from sickled blood are in better agreement with the calculated values based on grouped T_2 calibration for sickle blood[42] (blue line) than with those for normal blood[39,51] (red and magenta lines), with volunteer 3 being an exception. In contrast, the individually measured R_2 calibrations from normal blood do not show such large deviations from grouped T_2 calibrations (Supporting Information Fig. S2).

In Fig. 3, the calculated and measured Y for sickle blood samples were compared quantitatively. In terms of average performance over all of the blood samples, the calculated Y based on both the individual calibration and Bush-Wood's grouped calibration for sickle blood[42] correlated best with the measured Y (Figs. 3a and b), while the general T_2 calibrations for normal blood[39,51] underestimated Y by 13% (Fig. 3c) or 19% (Fig. 3d), respectively. In terms of individual measurements, the standard deviation (σ_Δ) of the difference between the measured and calculated Y based on the individual calibration was 0.030, which was half of the one between the measured and calculated Y based on the group calibration for sickle blood (σ_Δ : 0.062). Moreover, in the range of venous oxygenations ($Y<0.8$), σ_Δ of the individual T_2 calibrations was even smaller (0.015), compared to the 0.056 of the grouped calibration, showing a better agreement between measured and calculated Y values (Figs. 3a, b). This is very different from normal blood samples, in which the calculated Y values based on previous group calibrations for normal blood[39,51] showed good agreement and correlation with the measured individual Y values (Supporting Information Fig. S4).

To further explore the relationship between sickle blood T_2 and other hematological parameters, the two coefficients describing the Y dependence of sickle blood T_2 in Eq. 1 were fitted relative to Hct and the percentage of sickle hemoglobin in the total hemoglobin (HbS%) in Fig. 4. Coefficient A_1 of sickle blood (Fig. 4a), had a positive Hct-correlation similar to normal blood (r: 0.71 vs 0.61, respectively), but with a very different slope, namely 3–4 fold larger than that of normal blood (278 vs 79.9, respectively). Coefficient A_2 of sickle blood (Fig. 4b), had a very weak correlation with Hct ($r = -0.34$), while A_2 of normal blood had a strong positive correlation with Hct ($r = 0.93$). Meanwhile, although sickle blood samples had lower Hct, their A_2 values were generally higher than ones of normal blood. We also investigated the dependence of A_1 and A_2 on the HbS% for sickle

blood. To remove the interference of the A_1 dependence on Hct, A_2 was first scaled by Hct, then correlated with HbS%. Figs. 4c and d showed that neither A_1 nor Hct-scaled A_2 had any strong correlation with HbS%.

When determining ICC to assess reliability of our in vivo protocol[26] for measuring blood T_2 of SCA participants, we found a value of 0.986 (p-value < 0.00001), showing a high reliability. Using this protocol, T_2 values in the IJV were measured and converted to Y_v using several different T_2 calibrations for SCA participants (Table 1) and healthy participants (Supporting Information Table S1). As shown in Table 1, SCA participants' Y_v values obtained from the two T_2 calibrations for normal blood (0.504+/−0.071 and 0.447+/−0.105) were 18% and 26% lower than Y_v values obtained from individual calibrations (0.612+/−0.077). Bush-Wood's group calibration for sickle blood obtained an averaged Y_v value comparable to individual calibrations (0.625+/−0.053 vs 0.612+/−0.077), but Y_v values derived from these two calibrations sometimes still showed about 20% difference for some participants (#1 and #3). As a comparison, in healthy volunteers, Y_v values obtained from previous T_2 calibrations (0.603+/−0.058 and 0.637+/−0.062) were very close to Y_v values obtained from individual calibrations for every volunteer (0.610+/−0.062) (Supporting Information Table S1). Therefore, individual calibrations were used to calculate Y_v for SCA participants, and Bush-Wood normal blood calibrations were used for healthy volunteers.

Using the Y_v values determined for the IJV and the CBF values measured by PC-MRI, the whole-brain DO_2, OEF and $CMRO_2$ were calculated for SCA participants and healthy volunteers (Table 2). The Wilcoxon rank rum test showed that CBF of SCA participants (93.6+/−23.9 mL/min/100g) was significantly higher (p-value = 1.04×10^{-4}) than CBF of healthy volunteers (53.5+/−9.1 mL/min/100g), but DO_2 for SCA participants and healthy volunteers (457+/−57 vs 453+/−52 μmol/min/100g, p-value = 0.78) did not show a significant difference, and neither did OEF (0.375+/−0.075 vs 0.389+/−0.051, p-value = 0.31) and $CMRO_2$ (172+/−42 vs 174+/−17 μmol/min/100g, p-value = 0.73). Except for CBF (p-value < 0.01), correlations with Hct were not significant (p-values > 0.10) for any of the physiological parameters (DO_2, OEF or $CMRO_2$) either for SCA or healthy groups (Fig. 5).

Discussion

In this study, we evaluated both individual and group-based calibrations for the T_2-oxygenation relationships of sickled and normal blood. Our in vitro experiments demonstrated that for sickle blood Y calculation, T_2 calibrations built from sickle blood had better accuracy than those built from normal blood and that calibrating on sickle blood individually yielded higher precision than calibrating as a group (Figs. 2 and 3). When applying the individual calibrations to estimate the venous oxygenation of volunteers, no significant differences of OEF and $CMRO_2$ were observed between this group of SCA participants and healthy subjects.

Our in vitro measurement showed that T_2 values of sickle blood were mostly shorter than the ones based on normal blood's T_2 calibration at the same Hct (Fig. 2), confirming the findings of Bush et al.[42]. This phenomenon that HbS could induce shorter T_2 for the HbS

solution and sickle blood were also observed previously at lower magnetic field[46,54]. One reason for this could be that deoxygenated HbS tends to aggregate, and the aggregation of protein has been proven to induce a shorter water T_2 [55]. Meanwhile, the irregular shape of sickled erythrocyte may induce a stronger magnetic field gradient around the erythrocyte, which will further dephase the transverse magnetization of water diffusing around the erythrocyte and induce stronger T_2 relaxation; however, we did observe one subject (SCA volunteer 3 in Fig. 2) whose sickle blood T_2 values were close to the calculations based on the normal blood calibration. Such an occasional observation, similar to one measurement in a previous study[38], illustrates the diversity of T_2-Y relationships, but is insufficient evidence that T_2 calibration of normal blood is suitable for the Y calculation of sickle blood.

Our in vitro data also showed that Bush-Wood's group T_2 calibration specific for sickle blood[42], which only considered the effect of Y, could not accurately obtain Y values for some of the sickle blood samples (Fig. 3b). This relatively large difference between the measured and calculated Y in some individuals thus hampers its general application for in vivo measurements. To test whether this difference could result from the different SCA populations between our and their study, we applied the model used in Bush-Wood's sickle blood calibration ($1/T_2 = A_1+A_2\times(1-Y)^2$ where A_1 and A_2 were constant for all the samples) to fit our data, and we still found relatively large differences for some blood samples (Supporting Information Fig S3), which is similar to the original Bush-Wood's sickle blood calibration (Fig. 3b). We also evaluated Bush-Wood's normal blood calibration[51] on our normal blood samples (Fig. 4Sb). The high agreement between the calculated and measured Y on all normal blood samples indicates that the large difference between the calculated and measured Y for some sickle blood samples most likely results from a high variation in the composition of sickle blood, especially the erythrocyte size[56–58] and hemoglobin aggregation[54]. Current molecular studies have shown that many factors such as HbF could retard the HbS aggregation and erythrocyte sickling, and thus prevent the extra T_2 relaxation from HbS. All these factors make it difficult to universally characterize the sickle blood T_2 with a dependence only on Hct and Y.

To mitigate the heterogeneity effect of sickled blood, we investigated the T_2-Y relationship in blood samples from each SCA participant separately (Fig. 2). Compared with the group calibration[42], the individual calibration more accurately converted measured T_2 values into Y values for each subject (Fig. 3). Especially for the venous oxygenation range ($Y<0.8$), individual calibration provided superior accuracy and precision for in vivo measurements. Note that sickle blood T_2 values of different subjects all displayed a very good quadratic dependence on deoxygenation (1-Y) (Eq. 1) as shown in Fig. 2. This roots in two facts: 1). The two main contributions of T_2 relaxation, exchange[59] and diffusion[56–58,60] mechanisms have a $(1-Y)^2$ dependence; 2). The extra T_2 relaxation induced by the HbS aggregation process was observed to have a dependence of (1-Y), with the power of 2–2.4 [54].

The individual calibration ($1/T_2 = A_1\times(1-Y)^2 + A_2$) can further decompose sickle blood T_2 into a proportionality constant for oxygenation dependence (term A_1) and oxygenation independence (A_2), which provides the opportunity to investigate the relationship between sickle blood T_2 and blood physiology. As shown in Fig. 4a, A_1 highly correlated with Hct both for sickle and normal blood, in line with the fact that Hct determines the amount of

hemoglobin that can be deoxygenated. The slope of the A_1 dependence on Hct was larger for sickle blood than for normal blood, indicating that HbS aggregation during deoxygenating increased T_2 relaxation of sickle blood[46,54]; however, A_1 of sickle blood did not depend on the percentage of HbS, even if we scaled A_1 by Hct and so removed its effect (Fig. 4c). HbS aggregation and variability in erythrocyte shape are complicated processes that may be affected by other factors, such as the percentage of HbF.

Fig. 4b shows the Hct dependence of the oxygenation independent term A_2, which represents the arterial blood R_2 (i.e. $1/T_2$). Unlike normal blood, A_2 of sickle blood showed an weak and negative correlation with Hct, which was similar to previous observation by Bush et al.[42]. This was unexpected, because the hemoglobin was the main source of T_2 relaxation of arterial blood and blood T_2 should be shorter with increasing Hct, as shown in normal blood. One possibility is that sickle blood contains a relatively high concentration of young erythrocytes (reticulocytes) which contain high molecular weight micro-organelles such as ribosomes, and these could shorten T_2 values[61] and thus affect the Hct dependence of arterial blood R_2 (A_2). This could also explain why sickle blood with low Hct had similar or even higher A_2 values than normal blood. Another possibility results from the byproducts of hemolysis releasing to the plasma. These byproducts, especially methemoglobin, could shorten plasma T_1[62–64] and, to a lesser extent, T_2 and induce this abnormal Hct dependence of A_2. However, as listed in Table 2, the methemoglobin levels of our SCA volunteers were low and thus should have relatively small effect on the blood T_2 values. Certainly, concentration changes of other serum proteins, such as higher level of methemalbumin and lower levels of haptoglobin and hemopexin in SCA patients[65,66], could also affect A_2. However, these serum proteins' concentrations are relatively low compared to albumin[65,67], so they may not have a significant effect on A_2 values.

Using our individual calibration, we found that OEF and $CMRO_2$ of these SCA participants without a history of stroke or recent transfusion were similar to the values of healthy people. This is consistent with a previous PET study[2], but different from the MR results from Jordan et al.[38], Juttukonda et al.[41] and Guilliams et al.[7], which found people with SCA to have higher OEF, and the results from Bush et al.[42] which found people with SCA to have lower OEF. Besides the choice of T_2 calibrations used in these studies, another reason could be the different SCA populations that these studies focused on. One of the hypotheses in this latter studies[38,41] was that OEF was compensating CaO_2 and CBF. The total $CMRO_2$ is a multiplication product of CaO_2, CBF and OEF (Eq. 4). The population with SCA generally had lower Hct, which limits the amount of oxygen that a unit volume of arterial blood can carry (CaO_2); however, OEF has to be elevated only if CBF cannot be further increased to maintain the oxygen metabolism in the brain. However, in our (Fig. 5a) and many other studies[2,4,7–9,68], cerebral autoregulation of the arteriolar radius was able to sufficiently increase CBF to compensate for the reduced CaO_2 and maintain the cerebral oxygen delivery (DO_2 in Table 1). This was very similar to other studies of non-SCA hypoxia, such as hemodilution[69,70] and hypoxic hypoxia[71]. When CBF can no longer compensate for the deficiency in oxygen delivery, OEF will increase as shown in stroke patients[72]. Meanwhile, possible arterial-venous shunting in SCA participants[73] may decrease OEF[74].

The most important result from our study is that T_2-based OEF and $CMRO_2$ can be determined correctly only from proper individual calibration for each patient. With the availability of our approach, these more accurate values can now be used to further investigate the relationship between changes in OEF and $CMRO_2$ values and the risk of cerebral dysfunction and ischemia. Based on the stroke risk studies of non-SCA patients[75,76], OEF should be increased in response to reduced oxygen delivery secondary to anemia or stenosis and the $CMRO_2$ level should be maintained. However, the value of OEF as a potential indicator of increased risk of cerebral ischemia in SCA patients still need to be evaluated, due to different types of ischemia in SCA (chronic vs acute complications). Our work brings a non-invasive and convenient method to measure both OEF and $CMRO_2$, which supplies a powerful noninvasive approach to study the meaning of OEF and $CMRO_2$ changes in the evolution of ischemia in SCA patients.

The findings from present work should be considered in view of several limitations. First, in the comparison of whole brain OEF and $CMRO_2$ between healthy and SCA participants, the two groups were not well matched in age and sex; however, based on previous studies[77–80], these age or sex-related changes have a small effect considering the limited age difference between our two groups (35 ± 7 yrs vs. 25 ± 7 yrs). Second, in the calculation of OEF, we assumed the arterial oxygenation fraction (Y_a) in the arterial blood as 0.98 for SCA participants. This was because our SCA participants did not have significant cardiopulmonary disease, and thus arterial oxygenation fraction should be normal, which was also observed by previous study[81] Third, the sample size of our study was modest, and because of the complexity of sickle cell disease, we observed slightly larger variation of OEF and $CMRO_2$ among SCA participants (Table 2). Fourth, our study did not record some important physiological parameters, such as the reticulocyte concentration to help us extrapolate a universal T_2 calibration for sickle blood. Fifth, our study mainly focused on the global OEF and $CMRO_2$, which may miss possible changes in local oxygen stress, especially in the white matter,[35] for which the blood volume to ratio is small[82,83]. However, our study, which establishes a more correct relationship between blood T_2 and oxygenation in SCA patients and demonstrates the applicability of T_2-oxymetry in SCA patients, can in the future be combined with T_2-based oximetry mapping techniques[29,30,32] to further investigate the local oxygen stress in SCA patients. Last, we did not track the morphologic change of the erythrocyte. It is well known that the erythrocyte shape affects the blood T_2 value,[56,84] and that the shape of the erythrocyte depends on pO_2 (i.e. low pO_2 leads to increased sickling, while exposure to atmospheric oxygen can cause some sickled cells to regain the biconcave shape). Therefore, tracking the shape is ideal to thoroughly study the T_2 property of sickle blood. However, missing the morphologic information may not affect the accuracy of our T_2-Y calibration curve. This is because the degree of sickling mainly depends on the blood contents and oxygenation. For our individual calibration method, the blood samples in the in vitro calibration experiment were the same as the in vivo experiment for each SCA volunteer. Therefore, these blood samples had the same erythrocyte shape dependence on the pO_2, i.e. the in vitro blood T_2 measured at each blood oxygenation (or pO_2) included the effect of erythrocyte sickling. In other words, the T_2-Y calibration curve from these in vitro experiments contained the information of erythrocyte sickling and could faithfully transfer blood T_2 to Y for each SCA participant as possible. Certainly, many other

factors such as temperature, pH and the concentration of 2,3-DPG could affect the sickling of the erythrocyte[85,86] and some of these parameters may change during the blood storage[87]. However, our storage protocol, which kept the blood sample at room temperature and finished the experiment the same day, and our in vitro experimental protocol, which measures blood T_2 at 37°C minimized the possibility of this occurring.

Conclusion

Our in vitro validation showed that sickle blood T_2 values not only depend on Hct and Y as normal blood, but also on other hematological factors. The use of individual (patient-based) calibrations minimized the effect of heterogeneity of sickle blood between different SCA patients and improved the accuracy of T_2-based oximetry to study the cerebral oxygen utilization of SCA patients. Using the individual calibration, the measured OEF and $CMRO_2$ of SCA participants without a history of stroke were found to be not significantly different from the values of healthy people, despite their largely elevated CBF. Thus, individual T_2-Y calibrations are likely to be needed, if these non-invasively determined physiological parameters are to be studied and ultimately used to indicate the danger of ischemia in SCA patients and the need for treatment.

Supplementary Material

Refer to Web version on PubMed Central for supplementary material.

Acknowledgments

Grant support: NIH: P41 EB015909 (PvZ); NIH: K25 HL145129 (WL); NIH: K25 HL121192 (QQ); NIH S10 OD021648; Scholar Award of American Society of Hematology (QQ); NIH: R01 MH084021 (HL)

Reference

1. Hurlet-Jensen AM, Prohovnik I, Pavlakis SG, Piomelli S. Effects of total hemoglobin and hemoglobin S concentration on cerebral blood flow during transfusion therapy to prevent stroke in sickle cell disease. Stroke. 1994;25(8):1688–1692. [PubMed: 8042222]
2. Herold S, Brozovic M, Gibbs J, et al. Measurement of regional cerebral blood flow, blood volume and oxygen metabolism in patients with sickle cell disease using positron emission tomography. Stroke. 1986;17(4):692–698. [PubMed: 3488606]
3. Prohovnik I, Pavlakis SG, Piomelli S, Bello J, Mohr JP, Hilal S. Cerebral hyperemia, stroke, and transfusion in sickle cell disease. Neurology. 1989;39:344. [PubMed: 2927641]
4. Prohovnik I, Hurlet-jensen A, Adams R, et al. Hemodynamic etiology of elevated flow velocity and stroke in sickle-cell disease. J Cereb Blood Flow Metab. 2009;29(4):803–810. [PubMed: 19209182]
5. Xu F, Li W, Liu P, et al. Accounting for the role of hematocrit in between-subject variations of MRI-derived baseline cerebral hemodynamic parameters and functional BOLD responses. Hum Brain Mapp. 2018;39:344. [PubMed: 29024300]
6. Watchmaker JM, Juttukonda MR, Davis LT, et al. T2-relaxation-under-spin-tagging (TRUST) and Arterial Spin Labeling MRI elucidate discrepant hemo-metabolic mechanisms underlying elevated oxygen extraction fraction (OEF) in moyamoya and sickle cell anemia (SCA) patients. 2017:11–13.
7. Guilliams KP, Fields ME, Ragan DK, et al. Red cell exchange transfusions lower cerebral blood flow and oxygen extraction fraction in pediatric sickle cell anemia. Blood. 2018;131(9):1012–1021. [PubMed: 29255068]

8. Strouse JJ, Cox CS, Melhem ER, et al. Brief report Inverse correlation between cerebral blood flow measured by continuous arterial spin-labeling (CASL) MRI and neurocognitive function in children with sickle cell anemia (SCA). Blood. 2006;108(1):379–382. [PubMed: 16537809]
9. Bush AM, Borzage MT, Choi S, et al. Determinants of resting cerebral blood flow in sickle cell disease. Am J Hematol. 2016;91(9):912–917. [PubMed: 27263497]
10. Wise R, Bernardi S, Frackowiak RSJ, Legg NJ, Jones T. Serial observations on the pathophysiology of acute stroke. The transition from ischaemia to infarction as reflected in regional oxygen extraction. Brain. 1983;106:197–222. [PubMed: 6600956]
11. Baron J, Bousser M, Comar D, Soussaline F, Castaigne P. Non invasive tomographic study of cerebral blood flow and oxygen metabolism in vivo: Potentials, limitations and clinical applications in cerebral ischemic disorders. Eur Neurol. 1981;20:273. [PubMed: 6973468]
12. Heiss W, Huber M, Fink GR, et al. Progressive derangement of periinfarct viable tissue in ischemic stroke. J Cereb Blood Flow Metab. 1992;12:193–203. [PubMed: 1548292]
13. An H, Liu Q, Chen Y, et al. Oxygen metabolism in ischemic stroke using magnetic resonance imaging. Transl Stroke Res. 2012;3:65–75. [PubMed: 24323755]
14. Leigh R, Knutsson L, Zhou J, van Zijl PC. Imaging the physiological evolution of the ischemic penumbra in acute ischemic stroke. J Cereb Blood Flow Metab. 2018;38(9):1500–1516. [PubMed: 28345479]
15. Donahue MJ, Achten E, Cogswell PM, et al. Consensus statement on current and emerging methods for the diagnosis and evaluation of cerebrovascular disease. J Cereb Blood Flow Metab. 2018;38(9):1391–1417. [PubMed: 28816594]
16. Vichinsky EP, Neumayr LD, Gold JI, et al. Neuropsychological dysfunction and neuroimaging abnormalities in neurologically intact adults with sickle cell anemia. Jama. 2010;303(18):1823–1831. [PubMed: 20460621]
17. Frackowiak RS, Lenzi GL, Jones T, Heather JD. Quantitative measurement of regional cerebral blood flow and oxygen metabolism in man using 15O and positron emission tomography: theory, procedure, and normal values. J Comput Assist Tomogr. 1980;4(6):727–736. [PubMed: 6971299]
18. Davis TL, Kwong KK, Weisskoff RM, Rosen BR. Calibrated functional MRI: Mapping the dynamics of oxidative metabolism. Proc Natl Acad Sci. 1998;95(4):1834–1839. [PubMed: 9465103]
19. An H, Lin W. Quantitative measurements of cerebral blood oxygen saturation using magnetic resonance imaging. J Cereb Blood Flow Metab. 2000;20(8):1225–1236. [PubMed: 10950383]
20. He X, Yablonskiy DA. Quantitative BOLD: Mapping of human cerebral deoxygenated blood volume and oxygen extraction fraction: Default state. Magn Reson Med. 2007;57(1):115–126. [PubMed: 17191227]
21. Christen T, Lemasson B, Pannetier N, et al. Evaluation of a quantitative blood oxygenation level-dependent (qBOLD) approach to map local blood oxygen saturation. NMR Biomed. 2011;24(4):393–403. [PubMed: 20960585]
22. Bulte DP, Kelly M, Germuska M, et al. Quantitative measurement of cerebral physiology using respiratory-calibrated MRI. Neuroimage. 2012;60(1):582–591. [PubMed: 22209811]
23. Gauthier CJ, Hoge RD. Magnetic resonance imaging of resting OEF and $CMRO_2$ using a generalized calibration model for hypercapnia and hyperoxia. Neuroimage. 2012;60(2):1212–1225. [PubMed: 22227047]
24. Xu F, Uh J, Liu P, Lu H. On improving the speed and reliability of T2-relaxation-under-spin-tagging (TRUST) MRI. Magn Reson Med. 2012;68(1):198–204. [PubMed: 22127845]
25. Lu H, Ge Y. Quantitative evaluation of oxygenation in venous vessels using T2-Relaxation-Under-Spin-Tagging MRI. Magn Reson Med. 2008;60(2):357–363. [PubMed: 18666116]
26. Qin Q, Grgac K, van Zijl PCM. Determination of whole-brain oxygen extraction fractions by fast measurement of blood T(2) in the jugular vein. Magn Reson Med. 2011;65(2):471–479. [PubMed: 21264936]
27. Jain V, Magland J, Langham M, Wehrli FW. High temporal resolution in vivo blood oximetry via projection-based T2 measurement. Magn Reson Med. 2013;70(3):785–790. [PubMed: 23081759]
28. Wright GA, Hu BS, Macovski A. Estimating oxygen saturation of blood in vivo with MR imaging at 1.5 T. J Magn Reson Imaging. 1991;1(3):275–283. [PubMed: 1802140]

29. Bolar DS, Rosen BR, Sorensen AG, Adalsteinsson E. QUantitative Imaging of eXtraction of oxygen and TIssue consumption (QUIXOTIC) using venular-targeted velocity-selective spin labeling. Magn Reson Med. 2011;66(6):1550–1562. [PubMed: 21674615]
30. Guo J, Wong EC. Venous oxygenation mapping using velocity-selective excitation and arterial nulling. Magn Reson Med. 2012;68(5):1458–1471. [PubMed: 22294414]
31. Krishnamurthy LC, Liu P, Ge Y, Lu H. Vessel-specific quantification of blood oxygenation with T2 -relaxation-under-phase-contrast MRI. Magn Reson Med. 2014;71(3):978–989. [PubMed: 23568830]
32. Alderliesten T, De Vis JB, Lemmers PMAA, et al. T2-prepared velocity selective labelling: A novel idea for full-brain mapping of oxygen saturation. Neuroimage. 2016;139:65–73. [PubMed: 27291495]
33. Oja JM, Gillen JS, Kauppinen RA, Kraut M, van Zijl PC. Determination of oxygen extraction ratios by magnetic resonance imaging. J Cereb blood flow Metab. 1999;19(12):1289–1295. [PubMed: 10598932]
34. An H, Lin W. Impact of intravascular signal on quantitative measures of cerebral oxygen extraction and blood volume under normo- and hypercapnic conditions using an asymmetric spin echo approach. Magn Reson Med. 2003;50(4):708–716. [PubMed: 14523956]
35. Fields ME, Guilliams KP, Ragan DK, Binkley MM. Regional oxygen extraction predicts border zone vulnerability to stroke in sickle cell disease. Neurology. 2018;90:e1134.
36. Fields ME, Guilliams KP, Ragan D, et al. Hydroxyurea reduces cerebral metabolic stress in patients with sickle cell anemia. Blood. 2019;133(22):2436. [PubMed: 30858231]
37. Miao X, Choi S, Tamrazi B, et al. Increased brain iron deposition in patients with sickle cell disease: an MRI quantitative susceptibility mapping study. Blood. 2018;132(15):1618–1622. [PubMed: 30045839]
38. Jordan LC, Gindville MC, Scott AO, et al. Non-invasive imaging of oxygen extraction fraction in adults with sickle cell anaemia. Brain. 2016;139:738–750. [PubMed: 26823369]
39. Lu H, Xu F, Grgac K, Liu P, Qin Q, van Zijl P. Calibration and validation of TRUST MRI for the estimation of cerebral blood oxygenation. Magn Reson Med. 2012;67(1):42–49. [PubMed: 21590721]
40. Watchmaker JM, Juttukonda MR, Davis LT, et al. Hemodynamic mechanisms underlying elevated oxygen extraction fraction (OEF) in moyamoya and sickle cell anemia patients. J Cereb Blood Flow Metab. 2018;38(9):1618–1630. [PubMed: 28029271]
41. Juttukonda MR, Lee CA, Patel NJ, et al. Differential cerebral hemometabolic responses to blood transfusions in adults and children with sickle cell anemia. J Magn Reson Imaging. 2019;49:466. [PubMed: 30324698]
42. Bush AM, Coates TD, Wood JC. Diminished cerebral oxygen extraction and metabolic rate in sickle cell disease using T2 relaxation under spin tagging MRI. Magn Reson Med. 2018;80(1):294. [PubMed: 29194727]
43. Dover GJ, Boyer SH, Charache S, Heintzelman K. Individual variation in the production and survival of F Cells in sickle-cell disease. N Engl J Med. 1978;299:1428. [PubMed: 101847]
44. Franco RS, Yasin Z, Palascak MB, Ciraolo P, Joiner CH, Rucknagel DL. The effect of fetal hemoglobin on the survival characteristics of sickle cells. Blood. 2006;108(3):1073–1076. [PubMed: 16861353]
45. Gillis P, Petö S, Moiny F, Mispelter J, Cuenod C. Proton transverse nuclear magnetic relaxation in oxidized blood: a numerical approach. Magn Reson Med. 1995;33(1):93–100. [PubMed: 7891542]
46. Cottam GL, Valentine KM, Yamaoka K, Waterman MR. The gelation of deoxyhemoglobin S in erythrocytes as detected by transverse water proton relaxation measurements. Arch Biochem Biophys. 1974;162(2):487–492. [PubMed: 4407362]
47. Foltz WD, Stainsby JA, Wright GA. T2 accuracy on a whole-body imager. Magn Reson Med. 1997;38(5):759–768. [PubMed: 9358450]
48. Sung K, Nayak KS. Design and use of tailored hard-pulse trains for uniformed saturation of myocardium at 3 Tesla. Magn Reson Med. 2008;60(4):997–1002. [PubMed: 18816833]
49. Liu P, Xu F, Lu H. Test-retest reproducibility of a rapid method to measure brain oxygen metabolism. Magn Reson Med. 2013;69(3):675–681. [PubMed: 22517498]

50. Liu P, Chalak LF, Krishnamurthy LC, et al. T1 and T2 values of human neonatal blood at 3 Tesla: Dependence on hematocrit, oxygenation, and temperature. Magn Reson Med. 2016;75(4):1730. [PubMed: 25981985]
51. Bush A, Borzage M, Detterich J, et al. Empirical model of human blood transverse relaxation at 3 T improves MRI T2 oximetry. Magn Reson Med. 2017;77:2364. [PubMed: 27385283]
52. Herscovitch P, Raichle ME. What is the correct value for the brain--blood partition coefficient for water? J Cereb Blood Flow Metab. 1985;5(1):65–69. [PubMed: 3871783]
53. Kety SS, Schmidt CF. The nitrous oxide method for the quantitative determination of cerebral blood flow in man: theory, procedure and normal values. J Clin Invest. 1948;27(4):476–483. [PubMed: 16695568]
54. Cottam GL, Waterman MR. Effect of oxygen concentration on trasnverse water proton relaxation times in erythrocytes homozygous and heterozygous for hemoglonin S. Arch Biochem Biophys. 1976;177(1):293–298. [PubMed: 187125]
55. Feng Y, Taraban MB, Yu YB. Water proton NMR - A sensitive probe for solute association. Chem Commun. 2015;51(31):6804–6807.
56. Kiselev VG, Novikov DS. Transverse NMR relaxation as a probe of mesoscopic structure. Phys Rev Lett. 2002;89(27):2–5.
57. Jensen JH, Chandra R. NMR relaxation in tissues with weak magnetic inhomogeneities. Magn Reson Med. 2000;44(1):144–156. [PubMed: 10893533]
58. Sukstanskii AL, Yablonskiy DA. Gaussian approximation in the theory of MR signal formation in the presence of structure-specific magnetic field inhomogeneities. J Magn Reson. 2003;163(2): 236–247. [PubMed: 12914839]
59. Luz Z, Meiboom S. Nuclear Magnetic Resonance Study of the Protolysis of Trimethylammonium Ion in Aqueous Solution—Order of the Reaction with Respect to Solvent. J Chem Phys. 1963;39(2):366.
60. Ziener CH, Kampf T, Jakob PM, Bauer WR. Diffusion effects on the CPMG relaxation rate in a dipolar field. J Magn Reson. 2010;202(1):38–42. [PubMed: 19853483]
61. Feng Y, Taraban MB, Yu YB. Water proton NMR-a sensitive probe for solute association. Chem Commun. 2015;51:6804–6807.
62. Matwiyoff NAA, Gasparovic C, Mazurchuk R, Matwiyoff G. The line shapes of the water proton resonances of red blood cells containing carbonyl hemoglobin, deoxyhemoglobin, and methemoglobin: implications for the interpretation of proton MRI at fields of 1.5 T and below. Magn Reson Imaging. 1990;8(3):295–301. [PubMed: 2366641]
63. Bass J, Sostman HD, Boyko O, Koepke JA. Effects of cell membrane disruption on the relaxation rates of blood and clot with various methemoglobin concentrations. Invest Radiol. 1990;25(11): 1232–1237. [PubMed: 2254058]
64. Li W, Grgac K, Huang A, Yadav N, Qin Q, van Zijl PCMM. Quantitative theory for the longitudinal relaxation time of blood water. Magn Reson Med. 2016;76(1):270–281. [PubMed: 26285144]
65. Reiter CD, Wang X, Tanus-Santos JE, et al. Cell-free hemoglobin limits nitric oxide bioavailability in sickle-cell disease. Nat Med. 2002;8(12):1383–1389. [PubMed: 12426562]
66. Hanson MS, Piknova B, Keszler A, et al. Methaemalbumin formation in sickle cell disease: Effect on oxidative protein modification and HO-1 induction. Br J Haematol. 2011;154(4):502–511. [PubMed: 21595649]
67. LATHEM W JENSEN WN. Plasma hemoglobin-binding capacity in sickle cell disease. Blood. 1959;14:1047. [PubMed: 14414438]
68. Juttukonda MR, Jordan LC, Gindville MC, et al. Cerebral hemodynamics and pseudo-continuous arterial spin labeling considerations in adults with sickle cell anemia. NMR Biomed. 2017;30(2):e3681.
69. Paulson OB, Parving HH, Olesen J, Skinhoj E. Influence of carbon monoxide and of hemodilution on cerebral blood flow and blood gases in man. J Appl Physiol. 1973;35(1):111. [PubMed: 4716144]

70. Daif AAA, Hassan YMAEM, Ghareeb, Nawal Abd El-Galil Othman MM, Mohamed SAM. Cerebral effect of acute normovolemic hemodilution during brain tumor resection. J Neurosurg Anesthesiol. 2012;24(1):19–24. [PubMed: 21904221]
71. Ainslie PN, Shaw AD, Smith KJ, et al. Stability of cerebral metabolism and substrate availability in humans during hypoxia and hyperoxia. Clin Sci. 2014;670:661–670.
72. Ibaraki M, Shinohara Y, Nakamura K, Miura S, Kinoshita F. Interindividual variations of cerebral blood flow, oxygen delivery, and metabolism in relation to hemoglobin concentration measured by positron emission tomography in humans. J Cereb Blood Flow & Metab. 2010;30(7):1296–1305. [PubMed: 20160738]
73. Dowling MM, Quinn CT, Ramaciotti C, et al. Increased prevalence of potential right-to-left shunting in children with sickle cell anaemia and stroke. Br J Haematol. 2017;176(2):300–308. [PubMed: 27766637]
74. Nahavandi M, Millis RM, Tavakkoli F, et al. Arterialization of peripheral venous blood in sickle cell disease. J Natl Med Assoc. 2002;94(5):320–326. [PubMed: 12069211]
75. Derdeyn CP, Videen TO, Yundt KD, et al. Variability of cerebral blood volume and oxygen extraction: Stages of cerebral haemodynamic impairment revisited. Brain. 2002;125(3):595–607. [PubMed: 11872616]
76. Grubb RL, Derdeyn CP, Fritsch SM, et al. Importance of Hemodynamic Factors in the Prognosis of Symptomatic Carotid Occlusion. J Am Med Assoc. 1998;280(12):1055–1060.
77. Peng S-L, Dumas JA, Park DC, et al. Age-related increase of resting metabolic rate in the human brain. Neuroimage. 2014;98(214):176–183. [PubMed: 24814209]
78. De Vis JB, Hendrikse J, Bhogal A, Adams A, Kappelle LJ, Petersen ET. Age-related changes in brain hemodynamics; A calibrated MRI study. Hum Brain Mapp. 2015;36(10):3973–3987. [PubMed: 26177724]
79. Pantano P, Baron J-CC, Lebrun-Grandie P, Duquesnoy N, Bousser M- GG, Comar D. Regional cerebral blood flow and oxygen consumption in human aging. Stroke. 1984;15(4):635–641. [PubMed: 6611613]
80. Yamaguchi T, Kanno I, Uemura K. Reduction in regional cerebral metabolic rate of oxygen during human aging. Stroke. 1986;17(6):1220–1228. [PubMed: 3492786]
81. Chai Y, Bush AM, Coloigner J, et al. White matter has impaired resting oxygen delivery in sickle cell patients. Am J Hematol. 2019;94:467. [PubMed: 30697803]
82. Lu H, Law M, Johnson G, Ge Y, Van Zijl PCMM, Helpern JA. Novel approach to the measurement of absolute cerebral blood volume using vascular-space-occupancy magnetic resonance imaging. Magn Reson Med. 2005;54(6):1403–1411. [PubMed: 16254955]
83. Wenz F, Rempp K, Brix G, et al. Age dependency of the regional cerebral blood volume (rCBV) measured with dynamic susceptibility contrast MR imaging (DSC). Magn Reson Imaging. 1996;14(2):157–162. [PubMed: 8847971]
84. Yablonskiy DA. Quantitation of intrinsic magnetic susceptibility-related effects in a tissue matrix. Phantom study. Magn Reson Med. 1998;39(3):417–428. [PubMed: 9498598]
85. Poillon WN, Kim BC. 2,3-Diphosphoglycerate and intracellular pH as interdependent determinants of the physiologic solubility of deoxyhemoglobin S. Blood. 1990;76(5):1028–1036. [PubMed: 2393711]
86. Eaton WA, Hofrichter J. Hemoglobin S gelation and sickle cell disease. Blood. 1987;70:1245. [PubMed: 3311198]
87. Asakura T, Hirota T, Nelson AT, Reilly MP, Ohene-Frempong K. Percentage of reversibly and irreversibly sickled cells are altered by the method of blood drawing and storage conditions. Blood Cells, Mol Dis. 1996;22(3):297–306. [PubMed: 9075581]

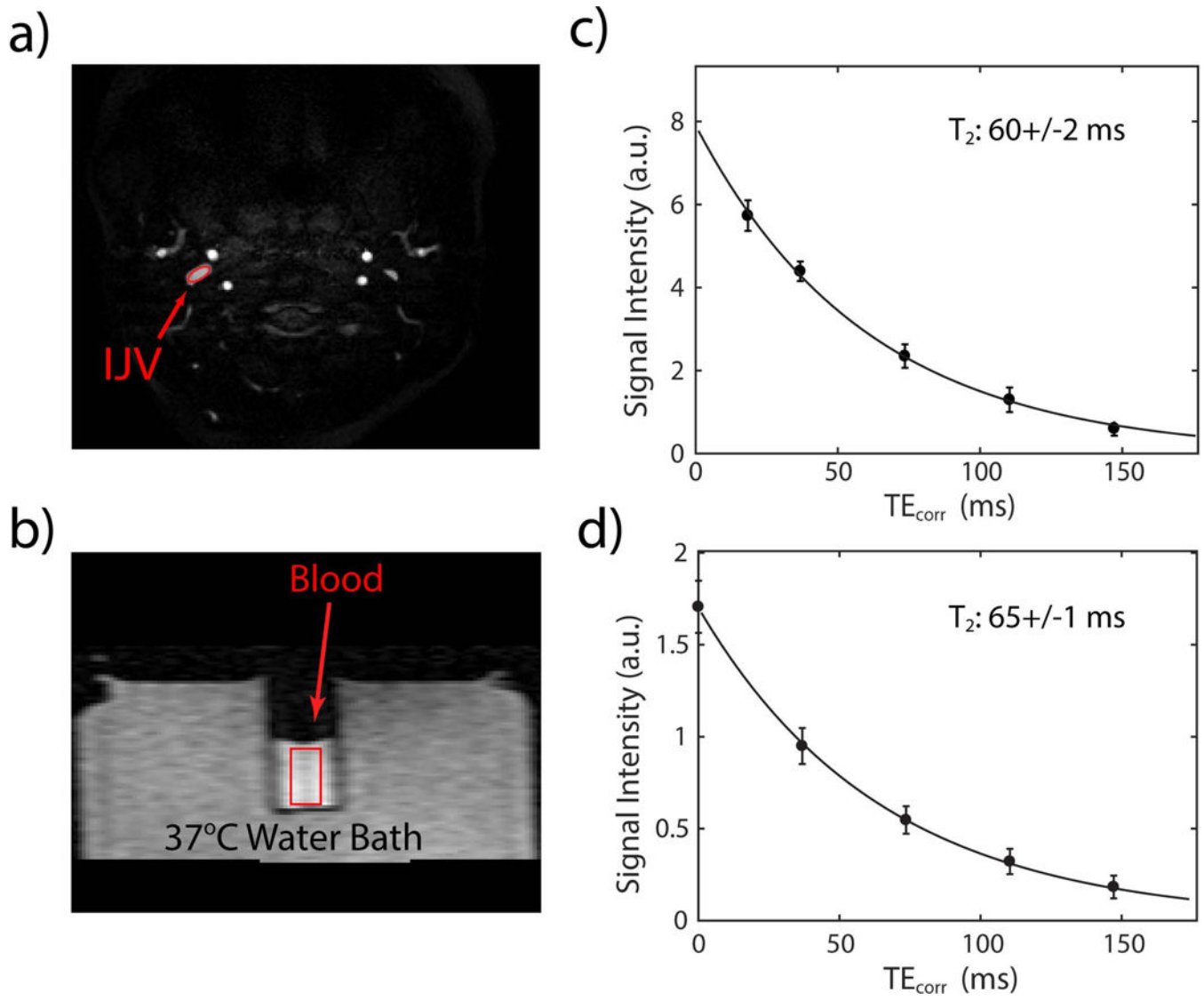

Figure 1.

In vivo and in vitro experiments to determine blood T_2 for one SCA participant. A representative image at the shortest TE_{corr} (a) in a slice through the IJV and (b) on a blood sample drawn from the same participant. The average intensities of each ROI (red) were fitted as a function of TE_{corr} using a single exponential decay function, $I = A \times \exp(-TE_{corr}/T_2)$, for the in vivo (c) and in vitro (d) experiments.

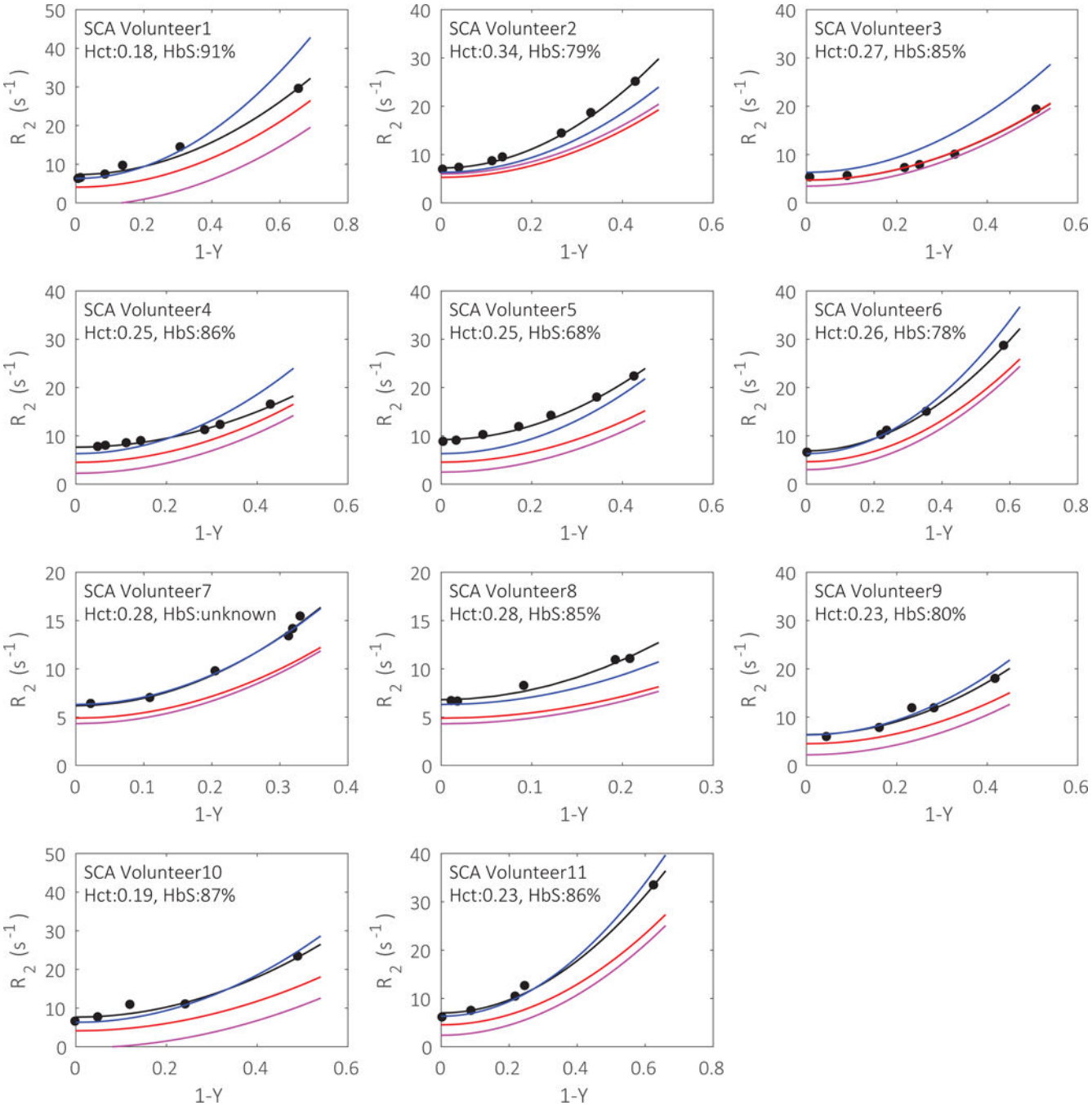

Figure 2.

The individual fittings (black lines) of sickle blood R_2 (black dots) as a function of oxygenations in samples from different SCA volunteers. The R_2-(1-Y) curves calculated using Bush-Wood's grouped calibration model from sickle blood (blue lines), Bush Wood's grouped calibration from normal blood (red lines) and Lu's grouped calibration from normal blood (magenta lines) are also shown.

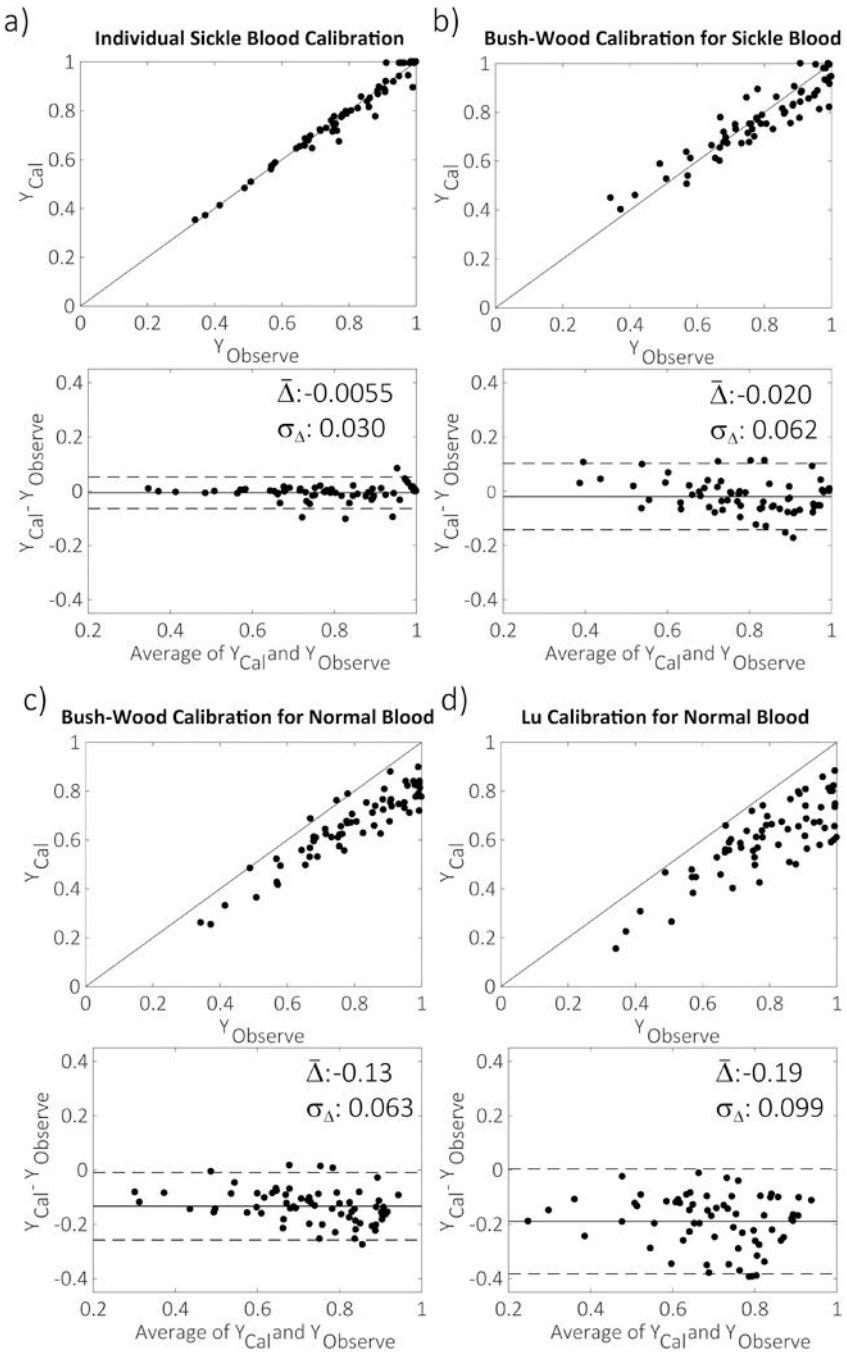

Figure 3.

The correlation and agreement (Bland-Altman) plots between the measured $Y_{Observe}$ of sickled blood samples from the blood analyzer and predicted Y_{cal} from four T_2-Y calibrations: (a) the individual calibration developed in this study; (b) Bush-Wood's group calibration for sickle blood c) Bush-Wood's group calibration for normal blood; (d) Lu's group calibration for normal blood; The average $\overline{\Delta}$ and standard deviation (σ_Δ) of the difference between predicted and measured Y are labeled in the plots. The dashed lines in the agreement plot represent two times the standard deviation from the mean difference.

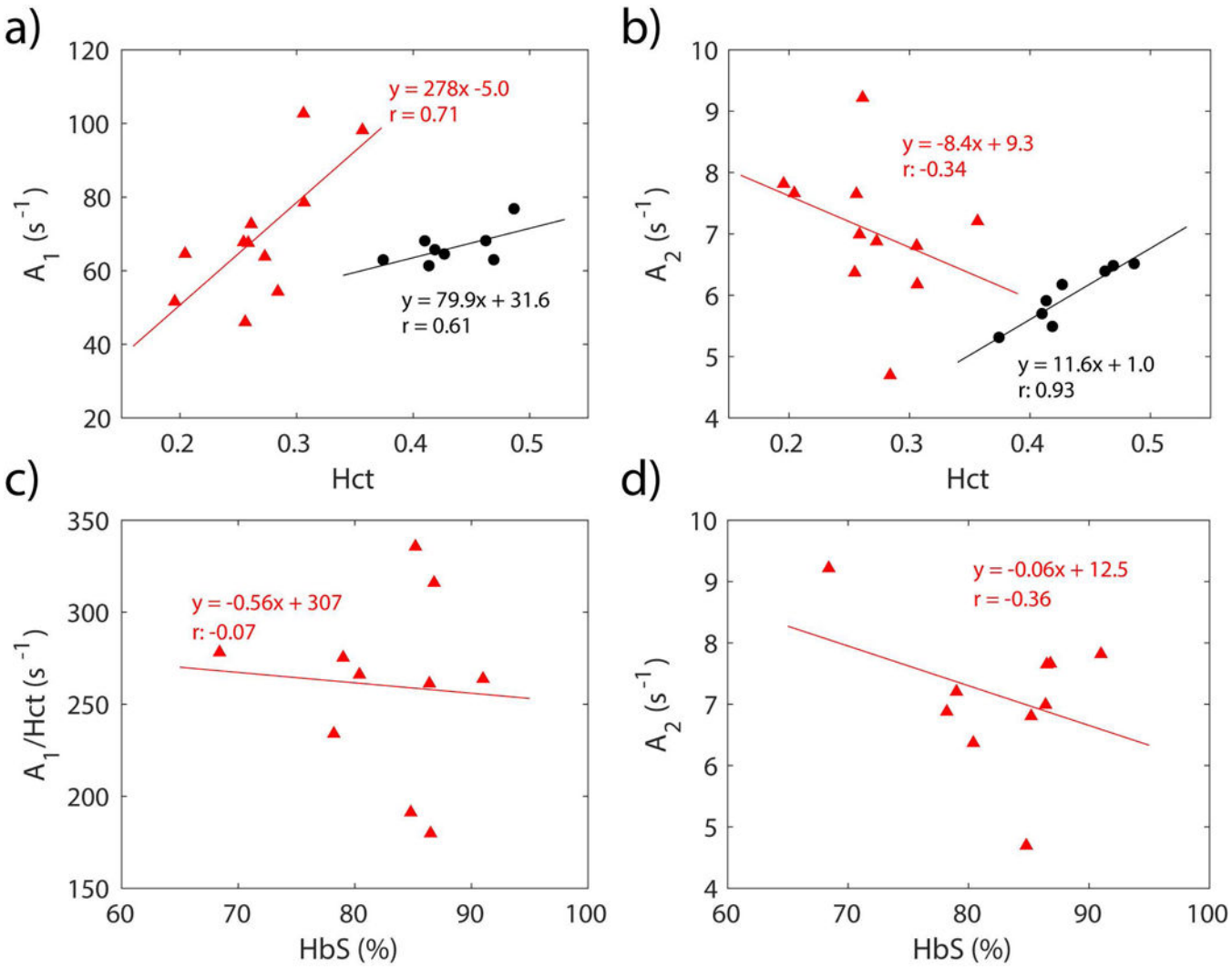

Figure 4.

The correlation of the coefficients A_1 (a,c) and A_2 (b,d) in the individual calculation (Eq. 1) with Hct and the percentage of sickle hemoglobin relative to the total hemoglobin (HbS%). The black dots represent A_1 and A_2 of each individual calibration from healthy volunteers, while the red dots represent A_1 and A_2 of each individual calibration from participants with SCA. The solid lines represent the linear fitting of the data and the correlation coefficients (r) are also given in the plot.

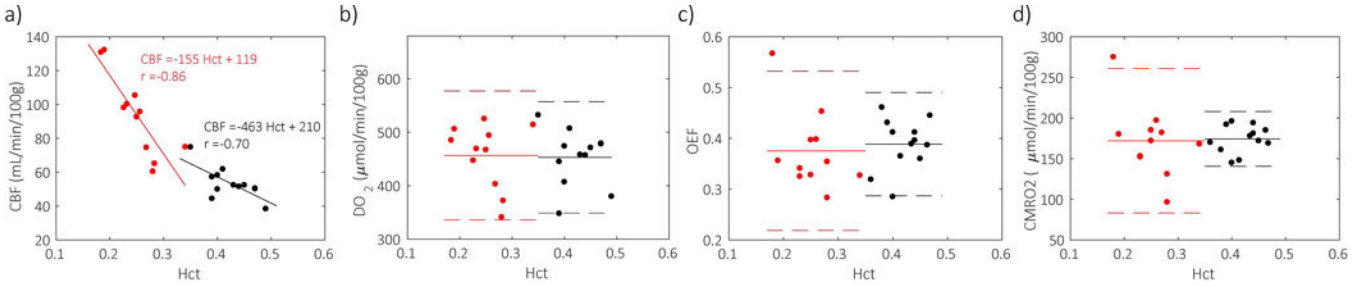

Figure 5:

Hct dependence of a) CBF, b) DO_2, c) OEF, and d) $CMRO_2$ for SCA participants (red) and healthy volunteers (black). In contrast to inverse correlations between Hct and CBF (a), no significant correlation between Hct and DO_2 (b), OEF (c), $CMRO_2$ (d) were observed. Linear fitting results were shown as solid lines for SCA participants (red) and healthy volunteers (black) in (a) while mean values of DO_2 (b), OEF (c) and $CMRO_2$ (d) were shown as solid lines with 95% confidence intervals (+/−1.96 standard deviation) as dash lines.

Table 1.

The calculated Y_v at IJV of each participant with SCA based on different T_2 calibrations. The numbers in the brackets show the normalized differences between the grouped calibrations and the individual calibrations.

		individual calibration	Bush-Wood's group calibration for sickle blood*	Bush-Wood's group calibration for normal blood*	Lu's group calibration for normal blood
Participants with SCA	1	0.43	0.51 (21%)	0.33 (−22%)	0.19 (−56%)
	2	0.66	0.60 (−8.9%)	0.52 (−21%)	0.54 (−19%)
	3	0.54	0.64 (20%)	0.53 (−0.7%)	0.50 (−6.2%)
	4	0.66	0.70 (6.5%)	0.59 (−10%)	0.53 (−19 %)
	5	0.59	0.55 (−6.3%)	0.43 (−28%)	0.38 (−36%)
	6	0.59	0.61 (3.9%)	0.50 (−15%)	0.46 (−22%)
	7	0.63	0.63 (−0.5%)	0.53 (−17%)	0.51 (−20%)
	8	0.70	0.65 (−7.5%)	0.55 (−22 %)	0.52 (−25%)
	9	0.66	0.68 (2.3%)	0.55 (−16%)	0.48 (−28%)
	10	0.63	0.64 (1.0%)	0.48 (−23%)	0.35 (−44 %)
	11	0.65	0.66 (1.6%)	0.53 (−18%)	0.45 (−30%)
Average+/−STD		0.61+/−0.08	0.63+/−0.05	0.50+/−0.07	0.45+/−0.10

* Our measured $T_{2,corr}$ values were converted based on Eq. 2 to $T_{2,app}$ that is suitable for Bush-Wood's and Lu's cablibrations for normal blood.

Table 2.

The calculated whole-brain CaO_2, CBF, DO_2, OEF, and $CMRO_2$ of SCA participants and normal volunteers.

		$T_{2.corr}$*	Hct	HbS(%)	HbF(%)	MetHb(%)	OEF***	CaO_2*	CBF*	DO_2*	$CMRO_2$*
	1	41	0.18	91.0	2.7	1.8	0.57	3.71	131	485	275
	2	54	0.34	79.0	14.2	1.8	0.33	6.87	74.9	514	168
	3	62	0.27	84.8	6.5	1.8	0.45	5.41	74.5	403	182
	4	77	0.25	86.5	6.5	1.5	0.33	4.98	105.3	525	172
Participants	5	47	0.25	68.4	4.8	1.9	0.40	5.04	92.6	467	185
with SCA	6	57	0.26	78.2	16.4	2.0	0.40	5.17	95.7	494	197
	7	60	0.28	**	**	1.9	0.35	5.71	65.1	372	131
	8	64	0.28	85.2	9.1	1.9	0.28	5.65	60.4	341	96.5
	9	71	0.23	80.4	11.9	2.1	0.33	4.68	100.2	469	152
	10	61	0.19	86.8	7.8	2.2	0.36	3.83	132.2	506	180
	11	65	0.23	86.4	7.5	2.7	0.34	4.56	98.1	447	153
Average ±STD		**60 ±10**	**0.27 ±0.04**	**82.7 ±6.4**	**8.7 ±4.3**	**2.0 ±0.3**	**0.38 ±0.08**	**5.06 ±0.85**	**93.6 ±23.9**	**457 ±57**	**172 ±42**
	1	58	0.40	**	**	**	0.41	8.31	58.2	474	196
	2	89	0.41	**	**	**	0.29	8.37	61.8	507	145
	3	84	0.35	**	**	**	0.32	7.26	74.8	532	170
	4	55	0.45	**	**	**	0.41	9.18	52.3	471	194
	5	51	0.39	**	**	**	0.46	8	44.4	348	161
Healthy	6	63	0.47	**	**	**	0.36	9.67	50.4	478	172
Volunteers	7	59	0.44	**	**	**	0.40	9.05	51.5	457	181
	8	57	0.39	**	**	**	0.43	7.94	57.2	445	192
	9	49	0.49	**	**	**	0.45	10.1	38.3	380	169
	10	67	0.4	**	**	**	0.37	8.31	49.9	407	148
	11	59	0.47	**	**	**	0.39	9.74	50.2	479	185
	12	60	0.43	**	**	**	0.39	8.93	52.4	458	178
Average +/ −STD		**63 ±12**	**0.42 ±0.04**	**	**	**	**0.39 ±0.05**	**8.74 ±0.85**	**53.5 ±9.1**	**453 ±52**	**174 ±17**

*The unit of $T_{2,corr}$, CaO_2, CBF, DO_2 and $CMRO_2$ are ms, μmol/mL, mL/min/100g, μmol/min/100g, and μmol/min/100g, respectively.

**The HbF and HbS data for SCA Participant 7 and all healthy volunteers were not obtained

***OEF of SCA participants is calculated based on Y_V obtained from individual calibration